

## Retraction

# Retracted: The Management of Energy Transformation through Laser Charging in WPT for 5G Application: Prediction Model of the In<sub>0.3</sub>Ga<sub>0.7</sub>As Solar Cell

### Wireless Communications and Mobile Computing

Received 1 August 2023; Accepted 1 August 2023; Published 2 August 2023

Copyright © 2023 Wireless Communications and Mobile Computing. This is an open access article distributed under the Creative Commons Attribution License, which permits unrestricted use, distribution, and reproduction in any medium, provided the original work is properly cited.

This article has been retracted by Hindawi following an investigation undertaken by the publisher [1]. This investigation has uncovered evidence of one or more of the following indicators of systematic manipulation of the publication process:

- (1) Discrepancies in scope
- (2) Discrepancies in the description of the research reported
- (3) Discrepancies between the availability of data and the research described
- (4) Inappropriate citations
- (5) Incoherent, meaningless and/or irrelevant content included in the article
- (6) Peer-review manipulation

The presence of these indicators undermines our confidence in the integrity of the article's content and we cannot, therefore, vouch for its reliability. Please note that this notice is intended solely to alert readers that the content of this article is unreliable. We have not investigated whether authors were aware of or involved in the systematic manipulation of the publication process.

Wiley and Hindawi regrets that the usual quality checks did not identify these issues before publication and have since put additional measures in place to safeguard research integrity.

We wish to credit our own Research Integrity and Research Publishing teams and anonymous and named external researchers and research integrity experts for contributing to this investigation.

The corresponding author, as the representative of all authors, has been given the opportunity to register their

agreement or disagreement to this retraction. We have kept a record of any response received.

### References

- [1] C. Wang, G. Li, I. Ali, H. Zhang, H. Tian, and J. Lu, "The Management of Energy Transformation through Laser Charging in WPT for 5G Application: Prediction Model of the In<sub>0.3</sub>Ga<sub>0.7</sub>As Solar Cell," *Wireless Communications and Mobile Computing*, vol. 2022, Article ID 5991154, 8 pages, 2022.

## Research Article

# The Management of Energy Transformation through Laser Charging in WPT for 5G Application: Prediction Model of the $\text{In}_{0.3}\text{Ga}_{0.7}\text{As}$ Solar Cell

Chengmin Wang <sup>1,2</sup>, Guangji Li <sup>1</sup>, Imran Ali <sup>1,3</sup>, Hongchao Zhang <sup>1</sup>, Han Tian <sup>2</sup>, and Jian Lu <sup>1</sup>

<sup>1</sup>School of Science, Nanjing University of Science and Technology, Nanjing 210094, China

<sup>2</sup>School of Digital Equipment, Jiangsu Vocational College of Electronics and Information, 213003, China

<sup>3</sup>Department of Physics, University of Agriculture, Faisalabad, Pakistan

Correspondence should be addressed to Jian Lu; lj6805@njjust.edu.cn

Received 6 December 2021; Revised 20 December 2021; Accepted 23 December 2021; Published 19 January 2022

Academic Editor: Mohammad Farukh Hashmi

Copyright © 2022 Chengmin Wang et al. This is an open access article distributed under the Creative Commons Attribution License, which permits unrestricted use, distribution, and reproduction in any medium, provided the original work is properly cited.

5G is the latest-generation network that powers the IoT in pace with energy transformation essentially demanded during the modern world, especially the wireless form. Laser charging means laser beam irradiance of the solar cell panel to generate the photovoltaic power, and its way belongs to the WPT (Wireless Power Transfer). During the process, uncertain and ungovernable factors affect the energy transfer of efficiency. We have chosen the  $\text{In}_{0.3}\text{Ga}_{0.7}\text{As}$  material as the semiconductor of the PV (photovoltaic) panel to enhance its photoelectric conversion efficiency. Nevertheless, during the PV processing, nonlinearity elements impact the prediction modelling, making it extremely difficult. This paper proposes a new forecasting model based on SVM (Support Vector Machine) which is drawn from SLT (Statistical Learning Theory). Since the forecast belongs to classification issue essentially, the main idea of SVM is extending the SLT dimensions. We used the kernel function for realization. The PV is done under the different conditions (constant temperature, gradient temperature, or various laser power). The gathered data is processed by MATLAB and the 3rd software: LIBSVM. Without the parameter optimization, the prediction accuracy of classification is 80% (32/40) against 100% (40/40). Considering that the experiment data have small quantity, further make the over 650 data size samples which are calculated by the formula to verify the model. Through the effect of a few random factors, the result still remains 80% or higher. The research work has resulted in a solution of a fast and precise prediction model in laser charging solar cell panel. It also revealed the implicit relationship between the factors of the PV.

## 1. Introduction

Nowadays, WPT (Wireless Power Transfer) plays a vital role in supplying power to enhance the electricity-driven devices' mobile capacity. Its essential contribution is no interconnecting wires. The Internet of Things (IoT) devices harvest their required energy from the aforementioned environmental sources; for example, RF energy harvesting provides key benefits in terms of being wireless and readily available in the form of transmitted energy (TV/radio broadcasting stations, mobile base stations, and handheld radios), low cost,

and small form factor implementation [1]. The battery-powered devices can harness wireless power from the electromagnetic field in the air [2] or PV (photovoltaic) by the power beaming [3]. Various WPT technologies have been developed so far, including inductive coupling, magnetic resonant coupling, CCPT (capacitive coupled power transfer), EM (electromagnetic) radiation, and laser power beaming, among others [2, 4]. Compared with other methods, firstly laser charge is suitable for a long-distance energy transfer of character. Secondly, it is suitable for its high energy density. Under the 5G application background, the laser

charging provides an autonomous, long-distance, wireless, and constant power supply to the IoT nodes in smart city scenarios [5]. The main disadvantage of laser charging is the low efficiency of the photoelectric conversion. According to the solar cell efficiency tables [6, 7], the average levels are under 40%.

The theoretical maximum conversion efficiency of the laser cell composed of semiconductor materials has its own upper limit. There is a corresponding relationship between the band gap and the maximum conversion efficiency. It can be seen that the larger the band gap is, the higher the corresponding maximum conversion efficiency is. Take the GaAs material as an example, the band gap is 1.42 eV, and the maximum conversion efficiency is more than 70%. However, materials with a larger band gap also correspond to a shorter wavelength of the best conversion laser, which is not conducive to long-distance propagation in the air. Therefore, in the material selection of a laser battery, the band gap width is small. A GaAs laser cell has the best conversion efficiency near 808 nm band, which is the highest single-junction conversion efficiency in laser cell research. However, the 808 nm wavelength has a high energy loss when propagating through the atmosphere, so it is rarely used for long-distance high-energy transmission.

At 300 K, the band gap of the solid solution varies with the ratio given below:

$$E_g(x) = 0.354 + 0.604x + 0.475x^2 (\text{eV}), \quad (1)$$

where  $x$  means the ratio of the element In. When  $x = 0.3$ , the band gap energy of the  $\text{In}_{0.3}\text{Ga}_{0.7}\text{As}$  material is 1.01 eV, which is the ideal band gap for photoelectric conversion with a wavelength near 1000 nm, such as 1070 nm. Then, the atmospheric window is around 1000 nm while the corresponding bandgap is around 1.0 eV. The latter is small than the solar irradiation cell's band gap. According to the previous experiment data which were provided by the supplier (Shanghai Institute of Space Power-Sources [8] (Power-Sources, 2015 #1828)), compared with the other materials,  $\text{In}_{0.3}\text{Ga}_{0.7}\text{As}$  presented the better conversion efficiency near the 1070 nm band [9]. Therefore, we selected this material as the semiconductor material of the PV panel to enhance its photoelectric conversion efficiency.

Despite some additional solutions being carried out [10], the PV power generation has several problems in use. This paper provides forecasting of efficiency based on SVM (Support Vector Machine) to optimize the parameter of the system and then to feed the need.

The steady-state  $I$ - $V$  characteristics of a  $p$ - $n$  junction silicon solar cell are often described based on one diode model as [11]

$$I = -I_{\text{ph}} + I_o \left( e^{q(V-IR_s)/nkT} - 1 \right) + \frac{(V - IR_s)}{R_{\text{sh}}}, \quad (2)$$

where  $I_{\text{ph}}$  represents the photogenerated current,  $I_o$  is the reverse saturation current,  $q$  is the elementary charge,  $n$  is the ideality factor,  $k$  is the Boltzman constant,  $T$  is the

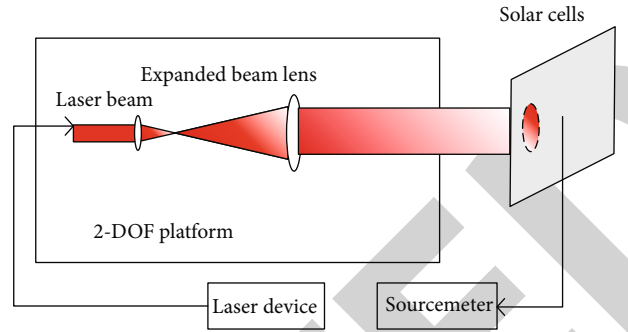


FIGURE 1: Schematic diagram of a laser charging device.

temperature of the cell,  $R_s$  is the series resistance of the silicon solar cell,  $R_{\text{sh}}$  is the shunt resistance, and  $I$  and  $V$  are the current and voltage of the module terminal, respectively.

As shown in Figure 1, the laser charging device, including the continuous laser device, beam expanding mirror, and 2-DOF platform, is connected with the active table in the corresponding solar panel to read the battery parameters and generate an  $I$ - $V$  curve [10].

Equation (2) indicates that  $I$  and  $V$  appear to be nonlinear, as shown in the experiment data in Figures 2 and 3 indicating the  $I$ - $V$  curves under the different laser irradiance.

Comparing Figures 2 and 3, the results of the experiment clearly revealed the  $I$ - $V$  curves' nonlinearity. However, the laser power irradiation level influences the max current and voltage especially the former. According to the PV power experiments, it was shown that the output values have been strongly correlated with inputs, such as solar irradiance, atmospheric temperature, module temperature, wind speed and direction, and humidity [12]. The solar panel irradiated by laser beam likewise has the effect under those environment conditions. The main challenge faced by those influence factors is the difficulty in building a normal forecasting model. Previous studies have reported that the power forecasting can be carried out without knowing the state of the environment by the use of the SVM [13]. SVM not only solves the nonlinear problems but also avoids the overfitting and trapping into the local minimum due to its convex optimization algorithm. This study tries to provide new insights into solving the nonlinearity power forecasting system.

ANN (artificial neural network) is widely used in forecasting the PV power generation in most research because of nonlinearity in meteorological data. ANN is more suitable compared with the statistical methods when a nonlinear and complicated bonding exists between the data without any prior assumption [12]. Here, SVM is well enough; in particular, we could not gather sufficient data to build the ANN prediction mode also avoiding being trapped into a mass computing crisis.

## 2. SLT (Statistical Learning Theory) and SVM

2.1. SLT Components. SVM is based on the SLT (Statistical Learning Theory) in the 1990s, which not only makes this theory an analytical tool but also makes a tool for creating practical algorithms for estimating multidimensional

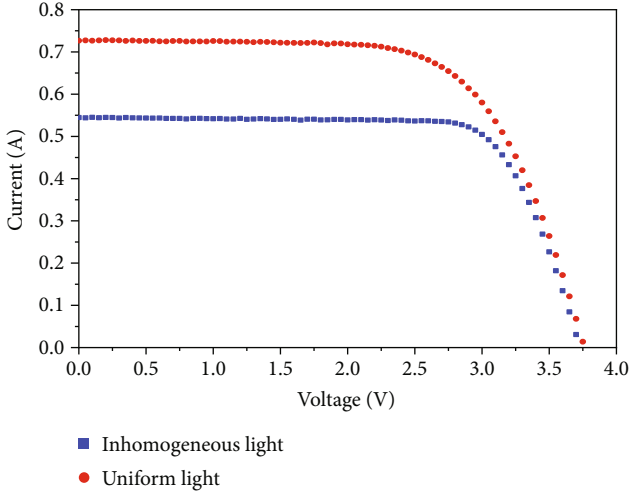


FIGURE 2:  $I$ - $V$  curves of the solar panel irradiated by 7.89 W laser power.

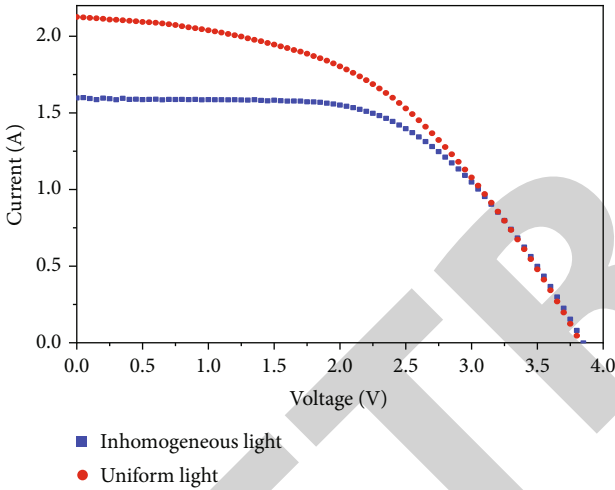


FIGURE 3:  $I$ - $V$  curves of the solar panel irradiated by 22.9 W laser power.

functions [14]. Its function approximates the Black Box. In facing an ill-posed problem with some explanation of empirical data, the SLT tries to build the instrument model for dealing with the truth.

The model based on SLT can be described using three components [14]:

- (1) A generator of a random vector  $x$ , drawn independently from a fixed but unknown distribution  $P_{(x)}$
- (2) A supervisor that returns an output vector  $y$  for every input vector  $x$ , according to a conditional distribution function  $P_{(y/x)}$ , also fixed but unknown
- (3) A learning machine capable of implementing a set of function  $f(x, a)$ ,  $a \in \Lambda$

Through training, choose the set of functions  $f(x, a)$ ,  $a \in \Lambda$ , from which the supervisor's response is predicted in

the best possible way. SLT suggests choosing from the set of rules ( $f(x, a)$ ,  $a \in \Lambda$ ), one that minimizes the number of misclassifications with the Black Box [15].

**2.2. The Evolution of the Risk Function.** A risk functional is given to an expected value of the loss between the answer to  $y$  of the input  $x$  and the response  $f(x, a)$  which resulted for the learning machine.

$$R(\alpha) = \int L(y, f(x, \alpha)) dP(x, y). \quad (3)$$

Equation (2)'s target is to minimize the risk functional  $R(a)$ . Despite the fact that the  $P(x, y)$  is unknown, the series of data  $(x_1, y_1), (x_2, y_2), (x_3, y_3), \dots, (x_n, y_n)$  are observed. Next, make the  $y$  as the output value only within  $[0, 1]$ ; consequently, the  $f(x, a)$ ,  $a \in \Lambda$ , is an indicator function as shown below:

$$L(y, f(x, a)) = \begin{cases} 0, & \text{if } y(x, a), \\ 1, & \text{else.} \end{cases} \quad (4)$$

Here, according to the regression function, get the loss function:

$$L(y, f(x, a)) = (y - f(x, a))^2. \quad (5)$$

The probability  $P(x, y)$  is unknown while the data  $(x_1, y_1), (x_2, y_2), \dots, (x_n, y_n)$  are observed. Let  $P(z)$  be the probability item defined on the space  $Z$ , and the corresponding function is  $Q(z, a)$ ,  $a \in \Lambda$ ; then, get the new minimization risk functional:

$$R(\alpha) = \int Q(z, \alpha) dP(z). \quad (6)$$

The probability measure  $P(z)$  is unknown, but the sample series data  $z_1, z_2, \dots, z_l$  are gotten. Then, variable  $z = (x, y) = (x^1, x^2, \dots, x^n, y)$  presents the  $n + 1$ -dimensional space vector.

$$R_{\text{emp}} \left( a = \frac{1}{l} \sum_{i=1}^l Q(z, a) \right). \quad (7)$$

**2.3. Empirical Risk Minimization (ERM).** Function (5) is replaced by the empirical risk function (6) which is called the ERM (Empirical Risk Minimization) principle. Since the ERM principle is a general formulation of these classical estimation problems, any theory concerning the ERM principle applies to the classical methods as well [14].

However, if the size of sample data was small,  $R_{\text{emp}}(a)$  could not insure the small value of risk. In the other words, the  $l$  is small; then, the  $R_{\text{emp}}(a_l)$  does not guarantee a small value of risk without the external principle. The second principle of SLT is SRM (structural risk minimization).

Let us roll back to component 3: function  $f(x, a)$ ,  $a \in \Lambda$ .  $S_1 \in S_2 \in \dots \in S_n$  where  $S_n$  is the subset of admissible functions

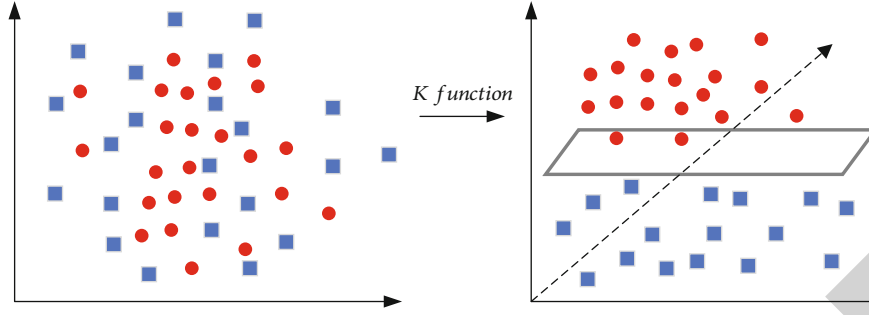
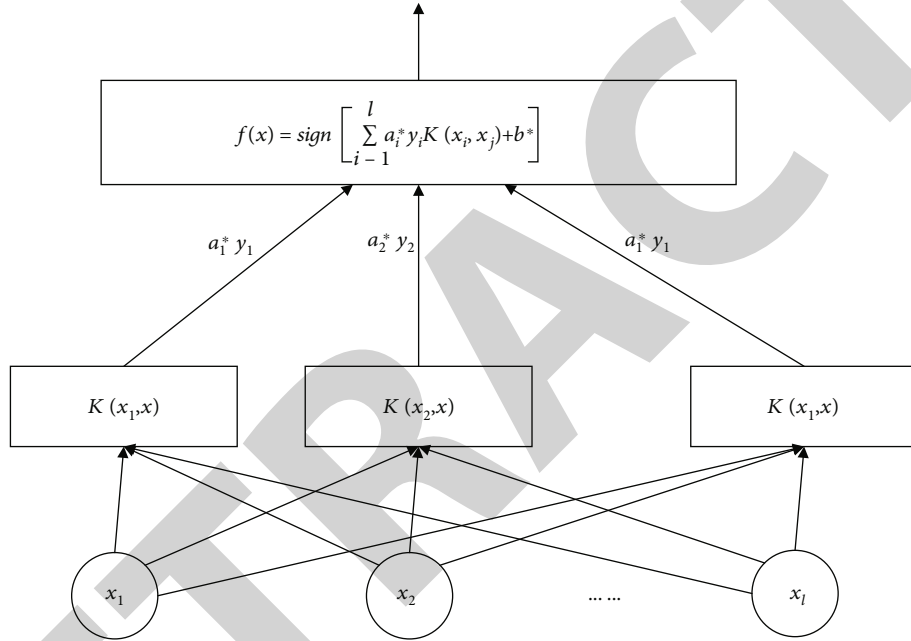
FIGURE 4: Expand SLT dimension from  $h$  to  $h + 1$ .

FIGURE 5: The structure of the SVM data flow.

with SLT dimension. There must be a suitable subset  $S_*$ , and its function  $f(x, a_0^*)$  is to minimize the value of the risk. This is the core idea of SRM, and its realization is what we called SVM technology.

**2.4. SVM expand SLT Dimension.** The SLT dimension  $h$  defined that  $h$  vectors cannot falsify the  $f(x, a), a \in \Lambda$ , and any  $h + 1$  vectors falsify the set [15]. The dimension means the complex of the function. The higher the dimension, the more complex the problem. Meanwhile, SVM concentrates on the SLT dimensions instead of the sample's dimensions, as shown in Figure 4.

The original is unable to classify data through the kernel function  $K$  for mapping the Hilbert space ( $H$ ) which is the optimal  $\Delta$ -margin separating hyperplane. The form is shown in Figure 5.

$$y = \text{sign} \left[ \sum_{i=1}^l a_i^* y_i K(x_i, x_j) + b^* \right]. \quad (8)$$

**2.5. SVM Kernel Function.**  $K$  means the kernel which has the inner product function. The kernel function of SVM ensures that the computation in the low-dimensional space is output to the high-dimensional space.  $K$  also corresponds to the neurons in the hidden layer. The output of the kernel, multiplied by the weight, goes to the activation function. The structure of SVM is the single layer of the neural network, as shown in Table 1.

The kernel function is  $K(x_i, x_j) = \varphi(x_i)^T \varphi(x_j)$ .

### 3. Experiments and Results

**3.1.  $\text{In}_{0.3}\text{Ga}_{0.7}\text{As}$  Solar Cell Schematic Diagram and Entity.** Now, we apply the SVM tool for generalization and regression prediction of the real WPT efficiency of the photoelectric conversion problems. The solar cell used in this experiment was a single-junction  $\text{In}_{0.3}\text{Ga}_{0.7}\text{As}$  solar cell fabricated by metal organic chemical vapor deposition (MOCVD) technology by the Shanghai Institute of Space Power-Sources. The schematic diagram of the solar cell is

TABLE 1: Classic SVM kernel functions.

Kernel	Form	Advantage	Disadvantage
Linear	$(x_i^T \cdot x_j)$	High efficiency	Unable to deal with a nonlinear task
Polynomial	$(\gamma x_i^T \cdot x_j + r)^d$	Solving nonlinearity	Too excess parameters
Radial basis	$\exp(-\gamma \ x_i - x_j\ ^2)$	Single parameter, mapping infinite dimension, training is extremely robust and efficient [16]	Calculate too slowly and risk of overfitting
Sigmoid	$\tanh(\gamma x_i^T \cdot x_j + r)$	Multilayer perceptron neural network	Poor effect, rarely used

\* $\gamma, r, d$  are kernel parameters.

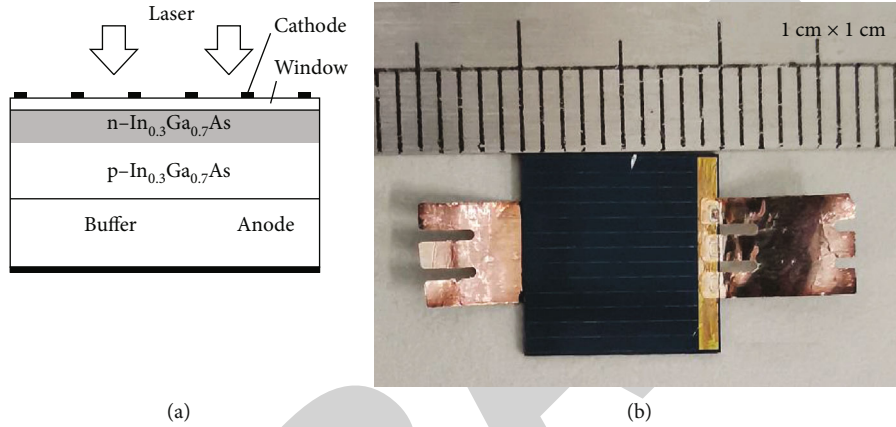


FIGURE 6: (a) Schematic diagram of the  $\text{In}_{0.3}\text{Ga}_{0.7}\text{As}$  solar cell and (b) the picture of the solar cell.

shown in Figure 6(a). The front surface was  $1 \text{ cm} \times 1 \text{ cm}$ , as shown in Figure 6(b), and the emitter region was  $n$ -doped, forming an  $np$ -type structure [17]. The subscript numbers present the ratio of the In or Ga element, as shown in Figure 6.

**3.2. Vectors of Experiments Selected.** The vectors of the experiment are listed: (1)  $I_{sc}$  (short-circuit current), (2)  $V_{oc}$  (open circuit), (3)  $P_{max}$  (max output power), (4)  $P_{laser}$  (laser light intensity), and (5)  $\eta$  (WPT efficiency). Those vectors' relationship can be expressed as follows:

$$\eta = \frac{I_{sc} \cdot V_{oc} \cdot FF}{P_{laser}}. \quad (9)$$

And FF means the fill factor:

$$FF = \frac{I_m \cdot V_m}{I_{sc} \cdot V_{oc}} = \frac{P_{max}}{I_{sc} \cdot V_{oc}}, \quad (10)$$

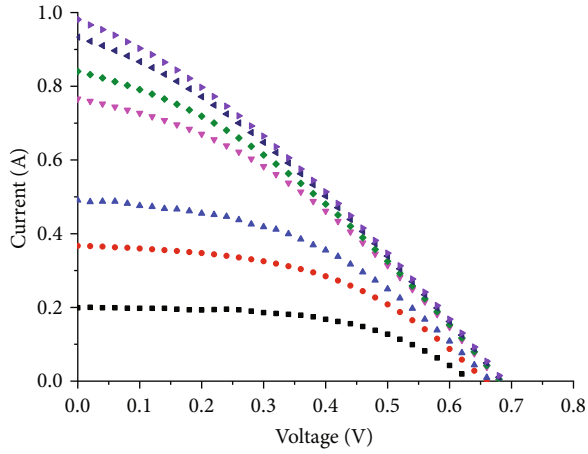
where  $I_m$  and  $V_m$  mean the current and voltage at the  $P_{max}$  which is the maximum power point.

**3.3. Gather Experiment Data under Different Conditions.**  $I$ - $V$  curve experiment data within four different conditions are shown in Figure 7.

**3.4. MATLAB Program and Running Results.** Those gathered data were transformed into .mat file style to be ready for the MATLAB software calculation. Most of users depend on the LIBSVM which is simple, easy-to-use, and efficient software for SVM classification and regression. It solves C-SVM classification, nu-SVM classification, one-class SVM, epsilon-SVM regression, and nu-SVM regression. It also provides an automatic model selection tool for C-SVM classification [18].

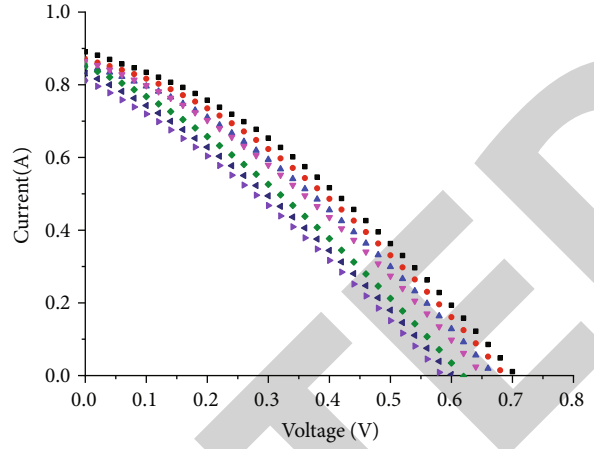
The LIBSVM coding needs a training set and testing set in the data; normally, we make half of the set to each other. The key problem in selecting kernel functions is dependent on the experience and the above describing the laser charging effective conditions: RBF function. The other parameters are not concerned with the issue; just set them to default, as shown in Figure 8.

The number of experiment data is 80, which is a too small-size sample to show typical and easy convergence. We make the over 650 data size sample which came from function (2) by Newton's method [19]. Function (2) belongs to the transcendental equation and presents the diode model which is most widely used. This model can be used to analyze the influence of five parameters on the performance of photovoltaic cells. Here, we utilized the function to calculate the  $I$ - $V$  curve by adjusting five parameters, without violating the scope of application of the model. The same LIBSVM model was used to test the accuracy, as shown in Figure 9.



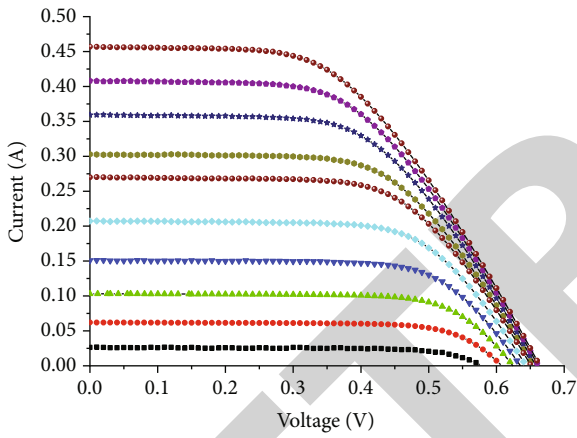
- 100 (mW/cm<sup>2</sup>)
- 200 (mW/cm<sup>2</sup>)
- ▲ 300 (mW/cm<sup>2</sup>)
- ▼ 400 (mW/cm<sup>2</sup>)
- ◆ 500 (mW/cm<sup>2</sup>)
- ◀ 600 (mW/cm<sup>2</sup>)
- ▶ 700 (mW/cm<sup>2</sup>)

Irradiation gradient laser power ( $\Delta P_{laser} = 100 \text{ mW/cm}^2$ ) under the constant temperature ( $T = 25^\circ \text{C}$ )



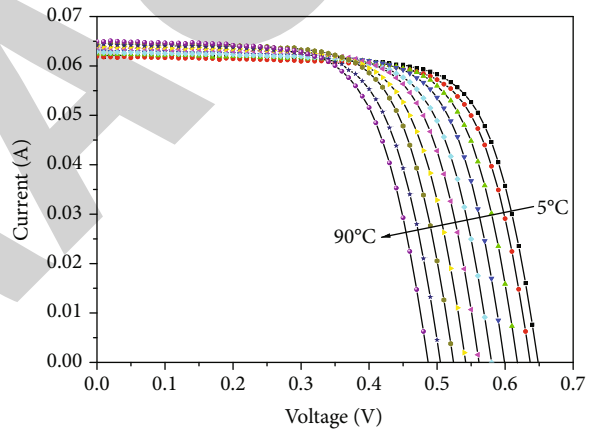
- 10°C
- 20°C
- ▲ 30°C
- ▼ 40°C
- ◆ 50°C
- ◀ 60°C
- ▶ 70°C

Irradiation gradient laser power ( $\Delta T = 10^\circ \text{C}$ ) under the same laser power  $P_{laser} = 100 \text{ mW/cm}^2$  temperature ( $T = 25^\circ \text{C}$ )



- 50
- 100
- ▲ 200
- ▼ 300
- ◆ 400
- ◀ 540
- ▶ 610
- ◀ 700
- ▶ 800
- ◀ 900

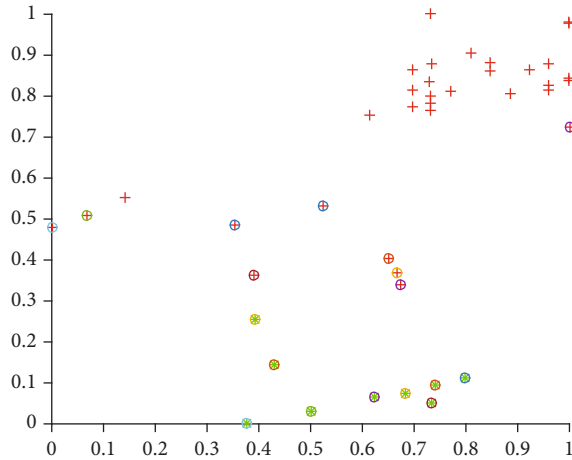
Irradiation differ laser power ( $P_{laser} \in [50, 900] \text{ mW/cm}^2$ ) under the constant temperature ( $T = 25^\circ \text{C}$ )



- 5°C
- 10°C
- ▲ 20°C
- ▼ 30°C
- ◆ 40°C
- ◀ 50°C
- ▶ 60°C
- ◀ 70°C
- ▶ 80°C
- ◀ 90°C

Irradiation differ laser power ( $T \in [5^\circ \text{C}, 25^\circ \text{C}]$ ) under the same laser power  $P_{laser} = 100 \text{ mW/cm}^2$  constant temperature ( $T = 25^\circ \text{C}$ )

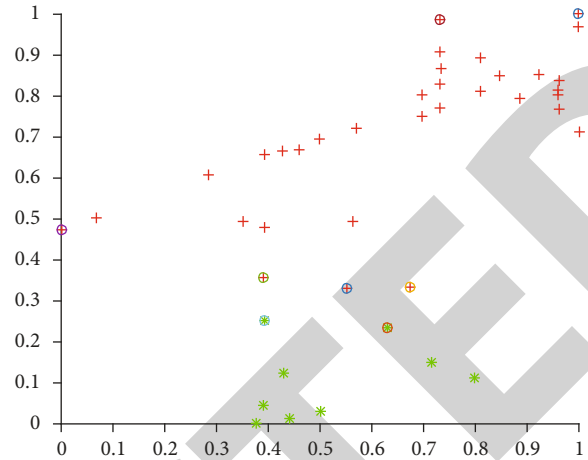
FIGURE 7: I-V curve experiment data within four different conditions.



The Accuracy = 80% (32/40) (classification).

Default parameters

- +
- \*
- 



Accuracy = 100% (40/40) (classification)

parameters optimization

FIGURE 8: Forecasting results (optimized or not) of laser charging calculation by LIBSVM in MATLAB.

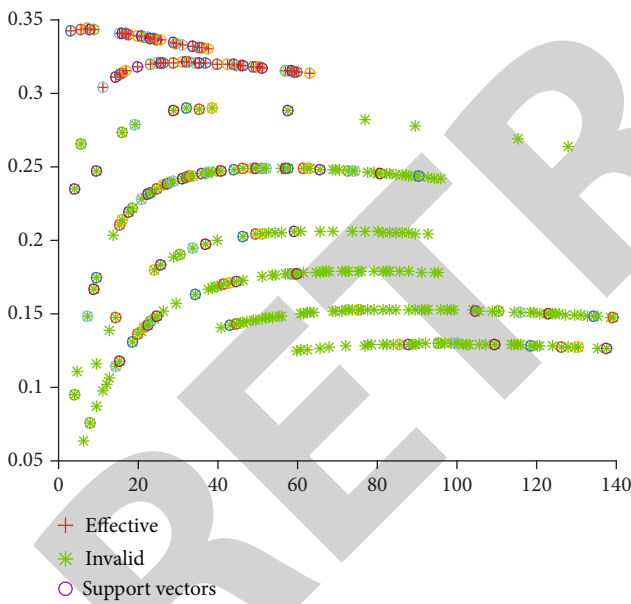


FIGURE 9: Examination of the forecasting results of laser charging calculation by LIBSVM in MATLAB.

The accuracy is basically about 80% or higher. The results demonstrate the forecasting model according to the experiment consequences. Above all, those MATLAB programs were running less than 60 seconds in normal PC.

#### 4. Discussion and Conclusions

In summary, this paper provided an effective SVM forecasting model for the laser charging. Despite the kinds of influence elements during the PV power experiment experience, the

prediction model shows the features of being extremely accurate and fast. The model is built by the small-size data which means it is easy to realize. Figures 8 and 9 show the support vectors, and the rule of the margin was observed obviously. Then, the model is not only binary but also multiclassification regression, which means that more WPT influence factors are considered. Future research should consider the potential effects of laser irradiance more carefully, and we observed that the phenomenon of the efficiency decreases with the increasing area of the solar cell. It might be the laser speckle's nonuniformity and then conducts even the wrong experiment data. During the laser charging time, we also discover that temperature impacts the power transferring efficiency (see Figure 7(d)). According to the conservation of energy, the most quantity of heat causing the raise in temperature is the transforming power lost. It is recommended how to reuse the energy to enhance the efficiency of the photoelectric conversion. With the 5G network developing, the energy supply of the IoT considers more high power and much long distance. The node of IoT also requires SWIPT (Simultaneous Wireless Information and Power Transfer), and the laser charging offers those demands' reality in the near future.

#### Data Availability

The datasets used and/or analyzed during the current study are available from the corresponding author on reasonable request.

#### Conflicts of Interest

The authors declared no potential conflicts of interest with respect to the research, authorship, and/or publication of this article.



## Acknowledgments

This work was supported by the National Defense Basic Scientific Research Program of China (No. JCKY2016606C002), the Shanghai Aerospace Science and Technology Innovation Fund (No. SAST20161113), and the National Natural Science Foundation of China (No. 11774176).

## References

- [1] P. Kamalinejad, C. Mahapatra, Z. Sheng, S. Mirabbasi, V. C. M. Leung, and Y. L. Guan, "Wireless energy harvesting for the Internet of things," *IEEE Communications Magazine*, vol. 53, no. 6, pp. 102–108, 2015.
- [2] Z. Zhang, H. Pang, A. Georgiadis, and C. Cecati, "Wireless power transfer—an overview," *IEEE Transactions on Industrial Electronics*, vol. 66, no. 2, pp. 1044–1058, 2019.
- [3] T. J. Nugent Jr. and J. T. Kare, "Laser power beaming for defense and security applications," in *SPIE Defense, Security, and Sensing*, vol. 8045, Orlando, Florida, United States, 2011.
- [4] Y. Zeng, B. Clerckx, and R. Zhang, "Communications and signals design for wireless power transmission," *IEEE Transactions on Communications*, vol. 65, no. 5, pp. 2264–2290, 2017.
- [5] A. Nguyen, P. M. Santos, M. Rosa, and A. Aguiar, "Study on solar-powered IoT node autonomy," in *2018 IEEE International Smart Cities Conference (ISC2)*, Kansas City, MO, USA, 2018.
- [6] M. Green, E. Dunlop, J. Hohl-Ebinger, M. Yoshita, N. Kopidakis, and X. Hao, "Solar cell efficiency tables (version 57)," *Progress in Photovoltaics*, vol. 29, no. 1, pp. 3–15, 2021.
- [7] M. A. Green, E. D. Dunlop, J. Hohl-Ebinger, M. Yoshita, N. Kopidakis, and X. Hao, "Solar cell efficiency tables (version 56)," *Progress in Photovoltaics*, vol. 28, no. 7, pp. 629–638, 2020.
- [8] Power-Sources, *S.I.o.S., Physics Power Technology*, Science Press, 2015.
- [9] N. A. Kalyuzhnyy, V. M. Emelyanov, V. V. Evstropov et al., "Optimization of photoelectric parameters of InGaAs metamorphic laser ( $\lambda=1064$  nm) power converters with over 50% efficiency," *Solar Energy Materials and Solar Cells*, vol. 217, article 110710, 2020.
- [10] C. Wang, G. Li, H. Zhang, and J. Lu, "The enhancement of the InGaAs solar cells by the thermoelectric generation technology under the continuous laser exposure," in *5th International Symposium on Laser Interaction with Matter*, Changsha, China, 2018.
- [11] M. L. Priyanka, M. Lal, and S. N. Singh, "A new method of determination of series and shunt resistances of silicon solar cells," *Solar Energy Materials and Solar Cells*, vol. 91, no. 2-3, pp. 137–142, 2007.
- [12] U. K. Das, K. S. Tey, M. Seyedmahmoudian et al., "Forecasting of photovoltaic power generation and model optimization: a review," *Renewable & Sustainable Energy Reviews*, vol. 81, pp. 912–928, 2018.
- [13] R. Xu, H. Chen, and X. Sun, "Short-term photovoltaic power forecasting with weighted support vector machine," in *2012 IEEE International Conference on Automation and Logistics*, Zhengzhou, China, 2012.
- [14] V. N. Vapnik, "An overview of statistical learning theory," *IEEE Transactions on Neural Networks*, vol. 10, no. 5, pp. 988–999, 1999.
- [15] V. Vapnik, "Universal learning technology: support vector machines," *NEC Journal of Advanced Technology*, vol. 2, no. 2, pp. 137–144, 2005.
- [16] N. Sujay Raghavendra and P. C. Deka, "Support vector machine applications in the field of hydrology: a review," *Applied Soft Computing*, vol. 19, pp. 372–386, 2014.
- [17] G. L. Guangji Li, H. Z. Hongchao Zhang, C. W. Chengmin Wang, Y. P. Yunxiang Pan, J. L. Jian Lu, and D. Z. Dayong Zhou, "Effect of 1070 nm laser intensity on parameters of In<sub>0.3</sub>Ga<sub>0.7</sub>As solar cell," *Chinese Optics Letters*, vol. 17, no. 3, article 031601, 2019.
- [18] C.-C. Chang and C.-J. Lin, "LIBSVM: a library for support vector machines," *ACM Transactions on Intelligent Systems and Technology*, vol. 2, no. 3, article 27, pp. 1–27, 2011.
- [19] S. Güttel and F. Tisseur, "The nonlinear eigenvalue problem," *Acta Numerica*, vol. 26, pp. 1–94, 2017.